# Apertureless near-field optical microscopy: Tip–sample coupling in elastic light scattering

Markus B. Raschke[a] and Christoph Lienau
*Max-Born-Institut für Nichtlineare Optik und Kurzzeitspektroskopie, Berlin, D-12489 Berlin, Germany*

(Received 12 June 2003; accepted 13 October 2003)

For linear light scattering in apertureless scanning near-field optical microscopy, we have studied the correlations between the tip radius of the probe, signal strength, spatial resolution, and sample material. Pronounced variations of the near-field distance dependence on tip shape and dielectric function of the sample are observed. For very sharp metal tips, the scattered near-field signal decays on a 5 nm length scale. Despite this highly localized tip–sample coupling, the contrast is found to depend sensitively on the vertical composition of the sample on a length scale given by the penetration depth of the incident light. The resulting implications on the use of the technique as an analytic probe method are discussed. © *2003 American Institute of Physics.*
[DOI: 10.1063/1.1632023]

Various efforts in optical microscopy have been devoted to overcome the classical diffraction limit by imaging in the optical near-field region. Most recently, the technique of so-called apertureless or scattering type scanning near-field optical microscopy ($s$-SNOM) showed great potential in this respect. Here, a metallic probe tip is illuminated and raster scanned in close proximity ($d \ll \lambda$) to the sample. The scattered light is collected in the far-field and high spatial resolution is obtained due to the local enhancement of the optical field at and near the sharp tip. With its virtues of superior resolution down to a few nm, access to a broad wavelength range and enhanced signal intensities render the technique advantageous over conventional fiber-tip-based methods.

Proposed theoretically for optical frequencies[1] and subsequently demonstrated experimentally,[2] the technique has since been taken in different directions ranging from linear vis[3–5] and IR scattering,[6] nonlinear two-photon fluorescence[7] and second-harmonic generation[8] to vibrational Raman spectroscopies.[9]

For linear light scattering, dielectric contrast with s-SNOM has recently been demonstrated in optical images.[3–5,10] It has been explained qualitatively by a coupled dipole model. However, despite the conceptual simplicity of the experiment, a number of parameters affect the scattering signal. Here, we address the influence of the tip shape, sample material, and its thickness on signal variation and the apparent contrast. It is found that the depth probed not only depends on the tip radius as suggested by the dipole model, but also on the vertical composition of the sample affecting the optical near field. This needs to be considered in the use of $s$-SNOM for material characterization.

In the experimental setup used, the probe tip is attached along one arm of a quartz tuning fork of an atomic force microscope. Careful measurements of the force–distance curves (width 12–16 nm) were used to establish a reference point for the imaging plane. A 2%–4% drop in the tuning fork signal defines the $d=0$ nm tip–sample distance with a relative accuracy of $\pm 2$ nm for the different tips and sample materials.

Light from a HeNe laser is focused onto the tip ($p$ polarized, $I=5$ mW, $\lambda=632.8$ nm, and $\theta=55°$). A near-diffraction limited spot of $\varnothing \approx 1.5$ $\mu$m is obtained using a high numerical aperture (NA) microscope objective (NA $=0.28$ and working distance$=30.5$ mm). The same objective is used in combination with a charge coupled device camera for visual tip inspection and to optimize the tip illumination.

Electrochemically etched tungsten tips were used.[11] Special emphasis is paid to a low vibration environment, optimized electrolyte concentration, and electrode potential, and the use of a fast switch-off circuit ensuring regularly shaped and smooth tips with tip radii $\lesssim 5$ nm as characterized by electron microscopy.

The optical signal is detected in the backscattered direction by a photodiode (New Focus, 2007) after spatial filtering. To discriminate the near-field signal from background scattering due to the tip and surface roughness, a modulation scheme is employed.[4,12,13] The tip is dithered harmonically in the $z$ direction with an amplitude comparable to or smaller than the tip radius ($z_0=2$–$5$ nm, and $f_z \sim 2$ kHz). The synchronized component of the optical signal at the fundamental or higher harmonic frequency is then detected by lock-in amplification.

Flat and carefully cleaned surfaces of different metals, semiconductors, and insulators were chosen for the investigation. To address the effect of the vertical sample composition, wedged gold films evaporated on glass, and silver samples coated with quartz of different thickness were used.

Figure 1(a) shows the total unmodulated tip-scattered signal during the approach of a flat gold sample. The tip–sample distance $d=0$ nm is defined by a 2%–4% drop in tuning fork signal. The undulation on the length scale of several 100 nm is due to interference. Possible pathways for pump or signal beams reaching tip or detector, respectively, with or without reflection from the surface are shown schematically in panel of Fig. 1(a). The overall increase of the signal is likely to be due to the all-constructive interference of the different contributions at $d=0$ nm.

[a]Electronic mail: raschke@mbi-berlin.de

 © 2003 American Institute of Physics
Downloaded 29 Aug 2005 to 62.141.169.241. Redistribution subject to AIP license or copyright, see http://apl.aip.org/apl/copyright.jsp

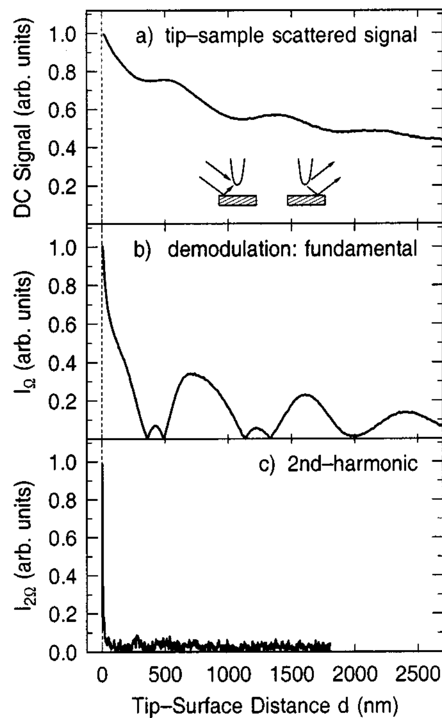


FIG. 1. Tip–sample distance dependence of near-field scattered light upon approach of a flat gold surface: (a) Total signal and (b) and (c) demodulated at the fundamental and second-harmonic of the $z$-modulation frequency $\Omega$, respectively.

Demodulation of the signal at the harmonics $n\Omega$, $n=1$, 2,... of the dither frequency discriminates the near-field contribution from the background (Figs. 1(b) and 1(c)).[5,13] The strong nonlinear distance dependence of the near-field tip–sample interaction enhances the corresponding high spatial frequency contributions, in particular those that exhibit variations on the length scale of the tip–dither amplitude. This leads to a steeper signal dependence for higher $n$.[13]

The correlation of the length scale of near-field coupling with the size of the tip apex is shown in Fig. 2. The normalized tip–sample distance dependence of $I_{2\Omega}$, i.e., the demodulated scattering signal at the second harmonic, is plotted for three tips with radii of curvature of $r\simeq 20$ nm, $r\simeq 12$ nm, and $r\lesssim 5$ nm. In this series, the stronger localization for sharper tips is accompanied by an overall signal increase by a factor of $\sim 20$.

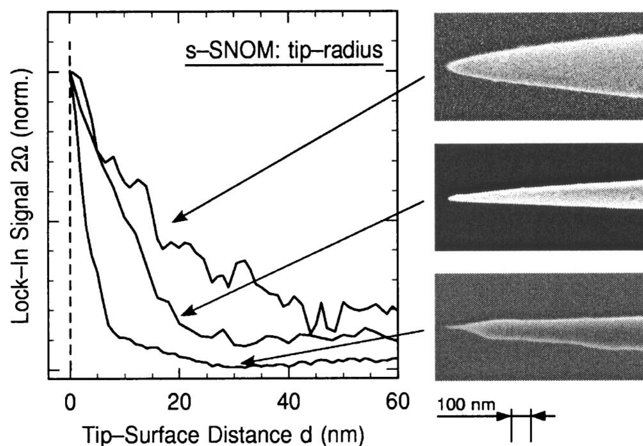


FIG. 2. Normalized tip–sample distance dependence of $I_{2\Omega}(d)$ for tips with different radii of curvature of $r\simeq 20$ nm, $r\simeq 12$ nm, and $r\lesssim 5$ nm. The ratio of $I_{2\Omega}(0$ nm) is 1:14:20 with the strongest signal for the $r\lesssim 5$ nm tip.

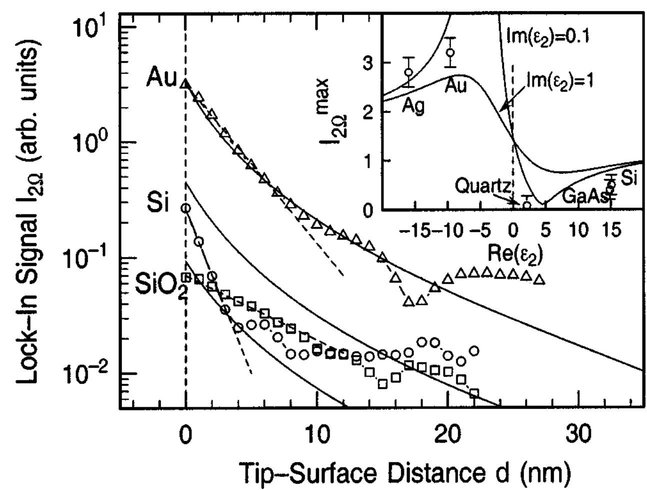


FIG. 3. Variation in optical amplitude $I_{2\Omega}(d)$ for different sample materials showing characteristic distance dependencies representative for metals, semiconductors, or insulators. Inset: $I_{2\Omega}^{\max}$ for. $d=0$ nm vs Re($\epsilon_2$) of the sample material. Solid lines correspond to a simple coupled dipole model.

Using a particular tip but different substrate materials, the resulting distance dependencies of $I_{2\Omega}(d)$ are shown in Fig. 3. In the inset of Fig. 3, the maximum signal intensities for $d=0$ nm are summarized and plotted as a function of the real part of the dielectric constant $\epsilon_2$ of the material. Both the shape of the distance dependencies—in particular the different initial slopes (dashed line)—as well as the variations of $I_{2\Omega}^{\max}$ at $d=0$ nm are found to be characteristic for the different classes of materials.

These results indicate a strong spatial localization of the tip–sample coupling, mostly determined by the tip geometry. To better understand the underlying mechanism for contrast formation and to address the degree of field localization inside the sample, we studied the effect of vertical composition on the scattered near-field signal. Figure 4 shows the dependence of the maximum scattered signal $I_{2\Omega}^{\max}$ ($d=0$ nm) on film thickness for a Au wedge evaporated on glass. The variation occurs on a much longer length scale than the tip–sample distance dependence which is plotted for comparison (solid line) in Fig. 4. In contrast, for Ag samples coated with thin quartz layers, the tip–distance $I_{2\Omega}(d)$ and quartz film thickness dependencies are found to correlate.

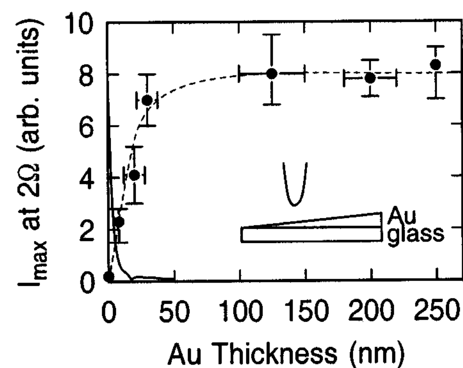


FIG. 4. Maximum signal amplitude $I_{2\Omega}^{\max}$ detected at $d=0$ for the gold wedge evaporated on quartz. The solid line shows the tip–sample distance dependence of the tip used.

Downloaded 29 Aug 2005 to 62.141.169.241. Redistribution subject to AIP license or copyright, see http://apl.aip.org/apl/copyright.jsp

To describe the experimental results, one frequently resorts to a simple model reducing the tip to a homogeneous sphere of radius $r$ and dielectric constant $\epsilon_1$, placed at distance $d$ in front of a half space representing the sample ($\epsilon_2$), and illuminated by a plane wave $E_0(\omega)$.[3,5,13] The induced dipole moment in the sphere $p_1$ can then be approximated by[14,15]

$$p_1=\alpha\{E_p+E_i(r+d)\}=\alpha\left\{E_p+\frac{\beta p_1}{2\pi[2(r+d)]^3}\right\}, \quad (1)$$

with the primary field $E_p$, the strength of the image field $E_i$ at the sphere location, the polarizability $\alpha$ of the sphere $\alpha=4\pi r^3(\epsilon_1-1)(\epsilon_1+2)^{-1}$, and the moment of the induced image dipole $\beta p_1=(\epsilon_2-1)(\epsilon_2+1)^{-1}p_1$ in the sample. Defining an effective polarizability of the coupled tip–sample system as $p_1\equiv\alpha_{\text{eff}}E_p$ results in

$$\alpha_{\text{eff}}=\alpha\left(1-\frac{\alpha\beta}{16\pi(r+d)^3}\right)^{-1}. \quad (2)$$

The mutual polarization of tip and sample thus enhance the optical near-field $E_{nf}\propto\alpha_{\text{eff}}E_p$ which is subsequently scattered by the tip. The near-field signal $I_s$ is directly proportional to the effective polarizability. It is given by $I_s\propto|E_{nf}+E_s|^2$ with $E_s$ representing background scattering by the tip. Scattering from residual surface roughness was found to be negligible. $I_s$ is then dominated in leading order by the term $(E_{nf}E_s^*+\text{c.c.})$.[13]

The solid line in Fig. 3 represents the calculated signal intensity $I_s$ as a function of tip–sample distance using $\epsilon_{\text{W}}=4.8+21.3i$ for the W sphere with radius 8 nm, $\epsilon_{\text{Au}}=-9.6+1.1i$, $\epsilon_{\text{Si}}=15.2+0.2i$, and $\epsilon_{\text{SiO}_2}=2.1$ (Ref. 16) for the different samples, respectively. Similarly, the expected variations of maximum signal amplitude are plotted in the inset of Fig. 3 as a function of $\text{Re}(\epsilon_2)$ with $\text{Im}(\epsilon_2)=0.1$ and 1 as parameters following the procedure described in Refs. 6 and 13.

The dipole model thus qualitatively accounts for the observed distance dependence and dielectric contrast with the near-field localized on a length scale determined by the tip radius. Yet, the experiments on the wedged gold film show that one is sensitive to variations in vertical sample composition on a much longer length scale of about 30 nm. To explain these long-range signal variations, one has to take into account that the primary field $E_p$ at the tip is due to both the direct illumination plus the Fresnel field from reflection from the surface. A similar argument holds for the scattered light $I_{2\Omega}$ reaching the detector. For metals, the Fresnel field intensity scales with film thickness given by the skin depth $\delta$, with $\delta=32$ nm for Au at $\lambda=633$ nm. In contrast, the thin quartz film on Ag has a negligible effect on the Fresnel coefficient for reflection. Quartz only weakly interacts with the tip and thus effectively acts only as a spacer layer between the tip and the metal.

However, the model fails to describe the exact form of the tip–distance dependence, e.g., the simple model neglects that, as the sample interacts with the large dipole near-field for reasons of symmetry, the presence of the sphere allows for the excitation of surface plasmons in the plane.[14] In addition, for small distances $d/r\lesssim1.5$,[17] the contributions from, e.g., quadrupole or higher-order moments, contribute to the polarization of the sphere. As a result of these higher-order poles, additional modes appear for the resonance of the coupled sphere–plane system.[2,14] These effects make the dielectric response depend on distance and might be responsible for the observed characteristic variations in slope for the different types of materials.

In summary, we have separated the spatial extent of the tip–sample near-field coupling from the influence of the vertical composition of the substrate contributing to the $s$-SNOM signal on two distinct length scales given by tip radius on the one hand, and light penetration depth on the other. This shows that by using a single optical frequency, the dielectric contrast can readily be obscured by vertical inhomogeneities of the sample. Here, spectrally resolved studies shall allow one to separate the influence of these different parameter and enable nanospectroscopy with true material specificity.

The authors gratefully acknowledge funding by the BMBF, stimulating discussions with T. Elsaesser, and invaluable assistance from F. Rust.

[1] J. Wessel, J. Opt. Soc. Am. B **2**, 1538 (1985).
[2] U. C. Fischer and D. W. Pohl, Phys. Rev. Lett. **62**, 458 (1989).
[3] F. Zenhausern, Y. Martin, and H. K. Wickramasinghe, Science **269**, 1083 (1995).
[4] Y. Inouye and S. Kawata, Opt. Lett. **19**, 159 (1994).
[5] R. Hillenbrand and F. Keilmann, Phys. Rev. Lett. **85**, 3029 (2000).
[6] R. Hillenbrand, T. Taubner, and F. Keilmann, Nature (London) **418**, 159 (2002).
[7] E. J. Sanchez, L. Novotny, and X. S. Xie, Phys. Rev. Lett. **82**, 4014 (1999).
[8] A. Bouhelier, M. Beversluis, A. Hartschuh, and L. Novotny, Phys. Rev. Lett. **90**, 013903 (2003).
[9] A. Hartschuh, E. J. Sánchez, X. S. Xie, and L. Novotny, Phys. Rev. Lett. **90**, 095503 (2003).
[10] R. Hillenbrand and F. Keilmann, Appl. Phys. Lett. **80**, 25 (2002).
[11] J. P. Ibe, P. P. Bey, S. L. Brandow, R. A. Brizzolara, N. A. Burnham, D. P. Dilella, K. P. Lee, C. R. K. Marrian, and R. J. Colton, J. Vac. Sci. Technol. A **8**, 3570 (1990).
[12] M. Labardi, S. Patanè, and M. Allegrini, Appl. Phys. Lett. **77**, 621 (2000).
[13] B. Knoll and F. Keilmann, Opt. Commun. **182**, 321 (2000).
[14] P. K. Aravind and H. Metiu, Surf. Sci. **124**, 506 (1983).
[15] R. Ruppin, Surf. Sci. **58**, 550 (1976).
[16] E. D. Palik, *Handbook of Optical Constants of Solids* (Academic, San Diego, 1985).
[17] R. Ruppin, Surf. Sci. **127**, 108 (1983).

**Downloaded 29 Aug 2005 to 62.141.169.241. Redistribution subject to AIP license or copyright, see http://apl.aip.org/apl/copyright.jsp**